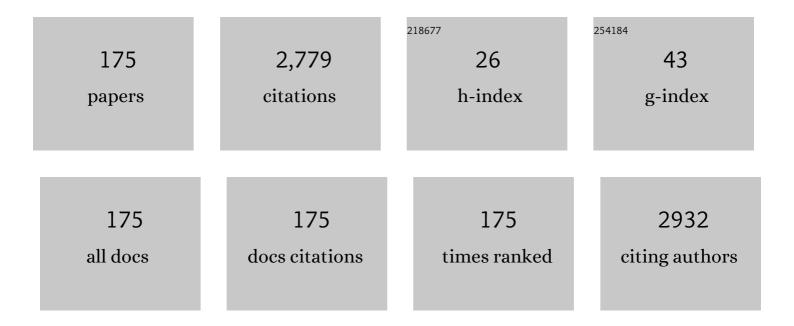
## Jerzy Morgiel

List of Publications by Year in descending order

Source: https://exaly.com/author-pdf/8046165/publications.pdf Version: 2024-02-01



#	Article	IF	CITATIONS
1	Microstructure and fracture toughness of Si3N4+graphene platelet composites. Journal of the European Ceramic Society, 2012, 32, 3389-3397.	5.7	151
2	A comparative study of the effect of mechanical and ultrasound agitation on the properties of electrodeposited Ni/Al2O3 nanocomposite coatings. Surface and Coatings Technology, 2012, 206, 2998-3005.	4.8	100
3	Microstructure and mechanical properties of the new Nb25Sc25Ti25Zr25 eutectic high entropy alloy. Materials Science & Engineering A: Structural Materials: Properties, Microstructure and Processing, 2016, 651, 590-597.	5.6	96
4	Hot pressed and spark plasma sintered zirconia/carbon nanofiber composites. Journal of the European Ceramic Society, 2009, 29, 3177-3184.	5.7	92
5	Effect of bilayer period on properties of Cr/CrN multilayer coatings produced by laser ablation. Surface and Coatings Technology, 2008, 202, 3501-3506.	4.8	69
6	Production of intermetallic compounds from Ti/Al and Ni/Al multilayer thin films—A comparative study. Journal of Alloys and Compounds, 2009, 484, 335-340.	5.5	67
7	Zirconia/carbon nanofiber composite. Scripta Materialia, 2008, 58, 520-523.	5.2	66
8	Nanoindentation of WC–Co hardmetals. Journal of the European Ceramic Society, 2013, 33, 2227-2232.	5.7	66
9	Effect of high-pressure torsion on grain refinement, strength enhancement and uniform ductility of EZ magnesium alloy. Materials Letters, 2018, 212, 323-326.	2.6	65
10	Electron Diffraction Based Analysis of Phase Fractions and Texture in Nanocrystalline Thin Films, Part III: Application Examples. Microscopy and Microanalysis, 2012, 18, 406-420.	0.4	64
11	XPS study of the cBN–TiC system. Ceramics International, 2001, 27, 637-643.	4.8	57
12	Deposition of Al2O3-TiO2 Nanostructured Powders by Atmospheric Plasma Spraying. Journal of Thermal Spray Technology, 2008, 17, 329-337.	3.1	57
13	Comparison of the Physicochemical Properties of TiO2 Thin Films Obtained by Magnetron Sputtering with Continuous and Pulsed Gas Flow. Coatings, 2018, 8, 412.	2.6	52
14	Silver nanocluster–silica composite coatings with antibacterial properties. Materials Chemistry and Physics, 2010, 120, 123-126.	4.0	50
15	Wear resistance of hot-pressed Si3N4/SiC micro/nanocomposites sintered with rare-earth oxide additives. Wear, 2010, 269, 867-874.	3.1	46
16	Direct observation of crystallization in silicon by in situ high-resolution electron microscopy. Ultramicroscopy, 1993, 51, 41-45.	1.9	44
17	Microstructure and Wear Behavior of Conventional and Nanostructured Plasma-Sprayed WC-Co Coatings. Journal of Thermal Spray Technology, 2010, 19, 964-974.	3.1	42
18	Microstructure of Ti3SiC2-based ceramics. Materials Letters, 1996, 27, 85-89.	2.6	41

#	Article	IF	CITATIONS
19	Microstructure of Fe–25Cr/(La, Ca)CrO3 composite interconnector in solid oxide fuel cell operating conditions. Materials Chemistry and Physics, 2003, 81, 434-437.	4.0	40
20	Ultrasound-assisted electrodeposition of Ni and Ni-Mo coatings from a citrate-ammonia electrolyte solution. Journal of Alloys and Compounds, 2017, 726, 410-416.	5.5	37
21	Crystallographic aspects related to advanced tribological multilayers of Cr/CrN and Ti/TiN types produced by pulsed laser deposition (PLD). Surface and Coatings Technology, 2006, 200, 6190-6195.	4.8	35
22	Screen-printed (La,Sr)CrO3 coatings on ferritic stainless steel interconnects for solid oxide fuel cells using nanopowders prepared by means of ultrasonic spray pyrolysis. Journal of Power Sources, 2012, 208, 86-95.	7.8	35
23	TEM analysis of surface layer of Ti-6Al-4V ELI alloy after slide burnishing and low-temperature gas nitriding. Applied Surface Science, 2020, 515, 145942.	6.1	34
24	New estimate of phase sequence in diffusive layer formed on plasma nitrided Ti-6Al-4V alloy. Surface and Coatings Technology, 2014, 259, 473-482.	4.8	33
25	Structural and mechanical aspects of multilayer graphene addition in alumina matrix composites–validation of computer simulation model. Journal of the European Ceramic Society, 2016, 36, 4171-4179.	5.7	30
26	Ti3SiC2 as a bonding phase in diamond composites. Journal of Materials Science Letters, 2001, 20, 1783-1786.	0.5	28
27	Microstructure and interfacial reactions in the bonding zone of explosively welded Zr700 and carbon steel plates. International Journal of Materials Research, 2015, 106, 782-792.	0.3	27
28	Indentation fatigue of WC–Co cemented carbides. International Journal of Refractory Metals and Hard Materials, 2013, 41, 229-235.	3.8	26
29	Mechanisms of the formation of low spatial frequency LIPSS on Ni/  Ti reactive multilayers. Journal Physics D: Applied Physics, 2016, 49, 365103.	2.8	26
30	Effect of heat treatment on magnetostructural transformations and exchange bias in Heusler Ni48Mn39.5Sn9.5Al3 ribbons. Acta Materialia, 2016, 103, 30-45.	7.9	26
31	Effect of Mo addition on corrosion of Zn coatings electrodeposited on steel. Corrosion Science, 2018, 135, 107-119.	6.6	26
32	Influence of rhenium addition on microstructure, mechanical properties and oxidation resistance of NiAl obtained by powder metallurgy. Materials Science & Engineering A: Structural Materials: Properties, Microstructure and Processing, 2018, 735, 121-130.	5.6	26
33	Oxidation and diffusion processes during annealing of TiSi(V)N films. Surface and Coatings Technology, 2015, 275, 120-126.	4.8	24
34	Long-range ordering kinetics and ordering energy in Ni3Al-based γ′ alloys. Intermetallics, 1993, 1, 139-150.	3.9	23
35	The effect of Mn partitioning in Fe–Mn–Si alloy investigated with STEM-EDS techniques. Materials Chemistry and Physics, 2003, 81, 466-468.	4.0	23
36	Microstructure and Strength of Al2O3 and Carbon Fiber Reinforced 2024 Aluminum Alloy Composites. Journal of Materials Engineering and Performance, 2014, 23, 2801-2808.	2.5	23

#	Article	IF	CITATIONS
37	BN sintered with Al: Microstructure and hardness. Ceramics International, 1997, 23, 89-91.	4.8	21
38	Thermal stability of nanoscale metallic multilayers. Thin Solid Films, 2014, 571, 268-274.	1.8	21
39	Effect of Nd doping on structure and improvement of the properties of TiO2 thin films. Surface and Coatings Technology, 2015, 270, 57-65.	4.8	21
40	Electron microscopy investigations of the cBN–Ti compound composites. Materials Chemistry and Physics, 2003, 81, 336-340.	4.0	20
41	Effect of nitriding conditions of Ti6Al7Nb on microstructure of TiN surface layer. Journal of Alloys and Compounds, 2020, 845, 156320.	5.5	20
42	Microstructure and Biocompatibility of Titanium Oxides Produced on Nitrided Surface Layer Under Glow Discharge Conditions. Journal of Nanoscience and Nanotechnology, 2011, 11, 8917-8923.	0.9	19
43	Modification of various properties of HfO2 thin films obtained by changing magnetron sputtering conditions. Surface and Coatings Technology, 2017, 320, 426-431.	4.8	19
44	Effect of reinforcement particle size on microstructure and mechanical properties of AlZnMgCu/AlN nano-composites produced using mechanical alloying. Journal of Alloys and Compounds, 2014, 586, S423-S427.	5.5	17
45	Phase transformations in Ni/Ti multilayers investigated by synchrotron radiation-based x-ray diffraction. Journal of Alloys and Compounds, 2015, 646, 1165-1171.	5.5	17
46	TEM examination of the effect of titanium on the Al/C interface structure. Materials Chemistry and Physics, 2003, 81, 319-322.	4.0	16
47	TEM characterization of the reaction products in aluminium–fly ash couples. Materials Chemistry and Physics, 2003, 81, 296-300.	4.0	16
48	Effect of low and high heating rates on reaction path of Ni(V)/Al multilayer. Materials Chemistry and Physics, 2017, 193, 244-252.	4.0	16
49	Enhanced thermal stability of a quasicrystalline phase in rapidly solidified Al-Mn-Fe-X alloys. Journal of Alloys and Compounds, 2017, 702, 216-228.	5.5	16
50	Microstructure Design and Tribological Properties of Cr/CrN and TiN/CrN Multilayer Films. Advanced Engineering Materials, 2008, 10, 617-621.	3.5	15
51	Amorphous FeCrNi/a-C:H coatings with self-organizednanotubular structure. Scripta Materialia, 2017, 136, 24-28.	5.2	15
52	Microstructure and wear of thermal sprayed composite NiAl-based coatings. Archives of Civil and Mechanical Engineering, 2019, 19, 1095-1103.	3.8	15
53	Effect of temperature on gas oxynitriding of Ti-6Al-4V alloy. Surface and Coatings Technology, 2019, 360, 103-109.	4.8	15
54	Postdeposition relaxation of internal stress in sputter-grown thin films caused by ion bombardment. Journal of Applied Physics, 1999, 85, 841-852.	2.5	14

#	Article	IF	CITATIONS
55	Interactions between molten aluminum and Y <sub>2</sub> O <sub>3</sub> studied with TEM techniques. Journal of Microscopy, 2010, 237, 253-257.	1.8	14
56	Influence of Nd dopant amount on microstructure and photoluminescence of TiO2:Nd thin films. Optical Materials, 2015, 48, 172-178.	3.6	14
57	Nanoparticles in zirconium-doped aluminide coatings. Materials Letters, 2015, 139, 50-54.	2.6	14
58	In-situ transmission electron microscopy observations of nucleation and growth of intermetallic phases during reaction of Ni(V)/Al multilayers. Thin Solid Films, 2017, 621, 165-170.	1.8	14
59	Multi-scale characterization and biological evaluation of composite surface layers produced under glow discharge conditions on NiTi shape memory alloy for potential cardiological application. Micron, 2018, 114, 14-22.	2.2	14
60	Arsenic-ion implantation-induced defects in HgCdTe films studied with Hall-effect measurements and mobility spectrum analysis. Infrared Physics and Technology, 2019, 98, 230-235.	2.9	14
61	Thin films of HgCdTe on silicon surfaces. Thin Solid Films, 1998, 318, 33-37.	1.8	13
62	Growth structure and growth defects in pulsed laser deposited Cr–CrNx–CrCxN1â^'x multilayer coatings. Surface and Coatings Technology, 2006, 200, 3644-3649.	4.8	13
63	Structure and properties of diffusive titanium nitride layers produced by hybrid method on AZ91D magnesium alloy. Transactions of Nonferrous Metals Society of China, 2014, 24, 2767-2775.	4.2	13
64	TEM investigations of active screen plasma nitrided Ti6Al4V and Ti6Al7Nb alloys. Surface and Coatings Technology, 2020, 383, 125268.	4.8	13
65	Hardness anisotropy and active slip systems in a (Hf-Ta-Zr-Nb)C high-entropy carbide during nanoindentation. International Journal of Refractory Metals and Hard Materials, 2021, 100, 105646.	3.8	13
66	Microstructure of boron nitride sintered with titanium. Materials Letters, 1995, 25, 49-52.	2.6	12
67	Microstructure of electrodeposited NiFe/Cu multilayers. Journal of Microscopy, 2010, 237, 456-460.	1.8	12
68	Detonation Deposited Fe-Al Coatings Part II: Transmission Electron Microscopy of Interlayers and Fe-Al Intermetallic Coating Detonation Sprayed onto the 045 Steel Substrate. Archives of Metallurgy and Materials, 2011, 56, 71-79.	0.6	12
69	D-gun Sprayed Fe-Al Single Particle Solidification. Archives of Metallurgy and Materials, 2014, 59, 211-220.	0.6	12
70	Microstructure and oxidation behaviour investigation of rhodium modified aluminide coating deposited on CMSX 4 superalloy. Journal of Microscopy, 2016, 261, 320-325.	1.8	12
71	Development of pore-free Ti-Al-C MAX/Al-Si MMC composite materials manufactured by squeeze casting infiltration. Materials Characterization, 2018, 146, 182-188.	4.4	12
72	The effect of Re addition on the thermal stability and structure of Ni–P electroless coatings. Materials Characterization, 2021, 171, 110811.	4.4	12

#	Article	IF	CITATIONS
73	Microstructure and properties of cold consolidated amorphous ribbons from (NiCu)ZrTiAlSi alloys. Journal of Alloys and Compounds, 2009, 483, 74-77.	5.5	11
74	Structural Characterization of Reaction Product Region in Al/MgO and Al/MgAl <sub>2</sub> 0 <sub>4</sub> Systems. Solid State Phenomena, 0, 172-174, 1273-1278.	0.3	11
75	Properties of Alumina Matrix Composites Reinforced with Nickel-coated Graphene. Materials Today: Proceedings, 2015, 2, 376-382.	1.8	11
76	TEM studies of low temperature cathode-plasma nitrided Ti6Al7Nb alloy. Surface and Coatings Technology, 2019, 359, 183-189.	4.8	11
77	AFM, XRD and HRTEM Studies οf Annealed FePd Thin Films. Acta Physica Polonica A, 2010, 117, 423-426.	0.5	11
78	Effect of deposition temperature on the morphology, structure, surface chemistry and mechanical properties of magnetron sputtered Ti70–Al30 thin films on steel substrate. Surface and Coatings Technology, 2001, 141, 252-261.	4.8	10
79	Reaction and diffusion phenomena upon oxidation of a (γ+α <sub>2</sub> ) TiAlNb alloy in air. Materials at High Temperatures, 2009, 26, 99-103.	1.0	10
80	Effect of silver on cellulose fibre colour. Coloration Technology, 2014, 130, 424-431.	1.5	10
81	Effect of the nanocrystalline structure type on the optical properties of TiO2:Nd (1at.%) thin films. Optical Materials, 2015, 42, 423-429.	3.6	10
82	Microstructure and positron lifetimes of zirconium modified aluminide coatings. Archives of Civil and Mechanical Engineering, 2018, 18, 1150-1155.	3.8	10
83	Thermal stability of plasma-sprayed NiAl/CrB2 composite coatings investigated through in-situ TEM heating experiment. Materials Characterization, 2020, 159, 110068.	4.4	10
84	Enhancement of fracture toughness of hot-pressed NiAl-Re material by aluminum oxide addition. Materials Science & Engineering A: Structural Materials: Properties, Microstructure and Processing, 2020, 790, 139670.	5.6	10
85	Nanoâ€īiC obtained through a reaction of MWCNTs with Zr(Y,Ti)O <sub>2</sub> . Journal of Microscopy, 2010, 237, 487-496.	1.8	9
86	Nanoparticles in hafnium-doped aluminide coatings. Materials Letters, 2015, 145, 162-166.	2.6	9
87	First stage of reaction of molten Al with MgO substrate. Materials Characterization, 2015, 103, 133-139.	4.4	9
88	Effect of Pd and Hf co-doping of aluminide coatings on pure nickel and CMSX-4 nickel superalloy. Archives of Civil and Mechanical Engineering, 2018, 18, 1421-1429.	3.8	9
89	Influence of low temperature plasma oxynitriding on the mechanical behavior of NiTi shape memory alloys. Vacuum, 2018, 156, 135-139.	3.5	9
90	On the TEM/EDS verification of Tu-Turnbull model of discontinuous dissolution. Scripta Metallurgica Et Materialia, 1994, 30, 1177-1181.	1.0	8

#	Article	IF	CITATIONS
91	Elastic TiN coating deposited on polyurethane by pulsed laser. Surface and Coatings Technology, 2006, 200, 6340-6345.	4.8	8
92	Relation between microstructure and hardness of nano-composite CrN/Si3N4 coatings obtained using CrSi single target magnetron system. Vacuum, 2013, 90, 170-175.	3.5	8
93	Characterization of Alumina Scale Formed on FeCrAl Steel. Archives of Metallurgy and Materials, 2014, 59, 77-81.	0.6	8
94	In-situ TEM heating of Ni/Al multilayers. International Journal of Materials Research, 2015, 106, 703-710.	0.3	8
95	TEM analysis of the hafnium-doped aluminide coating deposited on Inconel 100 superalloy. Vacuum, 2015, 116, 115-120.	3.5	8
96	Influence of pulsed current during high pressure sintering on crystallite size and phase composition of diamond with Ti B bonding phase. International Journal of Refractory Metals and Hard Materials, 2018, 70, 101-106.	3.8	8
97	Effect of Powder Preparation on the Microstructure and Wear of Plasma-Sprayed NiAl/CrB2 Composite Coatings. Journal of Thermal Spray Technology, 2019, 28, 1039-1048.	3.1	8
98	The Microstructure and Properties of Laser Shock Peened CMSX4 Superalloy. Metallurgical and Materials Transactions A: Physical Metallurgy and Materials Science, 2021, 52, 2845-2858.	2.2	8
99	A scanning photoemission microscope (SPEM) to study the interface chemistry of AlTi/C system. Journal of Materials Science Letters, 2000, 19, 123-126.	0.5	7
100	Characterization of interfaces in ZrO2–carbon nanofiber composite. Scripta Materialia, 2009, 61, 253-256.	5.2	7
101	Microstructure and hardness of Ti6Al4V/NiAl/Ti6Al4V joints obtained through resistive heating. Journal of Materials Processing Technology, 2018, 255, 689-695.	6.3	7
102	Influence of regulated modification of nitride layer by oxygen on the electrochemical behavior of Ti–6Al–4V alloy in the Ringer's solution. Materials and Corrosion - Werkstoffe Und Korrosion, 2019, 70, 2320-2325.	1.5	7
103	Quasi-amorphous, nanostructural CoCrMoC/a-C:H coatings deposited by reactive magnetron sputtering. Surface and Coatings Technology, 2019, 378, 124910.	4.8	7
104	Perforated alumina templates as a tool for engineering of CoPd film magnetic properties. Journal of Magnetism and Magnetic Materials, 2019, 477, 182-189.	2.3	7
105	In-situ investigation of phase transformations during heating of AlCoCrCuNi high entropy melt-spun ribbons. Materials Characterization, 2019, 148, 134-141.	4.4	7
106	Microstructure and Wear of (CrN/CrAlN)/(CrAlN/VN) and (CrN/TiAlN)/(TiAlN/VN) Coatings for Molds Used in High Pressure Casting of Aluminum. Coatings, 2020, 10, 261.	2.6	7
107	In situ TEM observation of reaction of Ti/Al multilayers. Archives of Civil and Mechanical Engineering, 2017, 17, 188-198.	3.8	6
108	The effect of post-process annealing on optical and electrical properties of mixed HfO2–TiO2 thin film coatings. Journal of Materials Science: Materials in Electronics, 2019, 30, 6358-6369.	2.2	6

#	Article	IF	CITATIONS
109	Wetting and interfacial reactivity of Ni–Al alloys with Al2O3 and ZrO2 ceramics. Journal of Materials Science, 2021, 56, 7849-7861.	3.7	6
110	Microstructure and Hardness of cBN–Zr Composite. Journal of the European Ceramic Society, 1998, 18, 389-393.	5.7	5
111	SEM and HRTEM study of zirconium-based glass forming alloys cast at various cooling rates. Materials Chemistry and Physics, 2003, 81, 376-379.	4.0	5
112	TEM investigation of ductile iron alloyed with vanadium. Journal of Microscopy, 2010, 237, 461-464.	1.8	5
113	Tem Investigation of Phases Formed During Aluminium Wetting of MgO at [100], [110] and [111] Orientations. Archives of Metallurgy and Materials, 2013, 58, 497-500.	0.6	5
114	Atomic scale structure investigations of epitaxial Fe/Cr multilayers. Applied Surface Science, 2014, 305, 154-159.	6.1	5
115	Influence of the structural and surface properties on photocatalytic activity of TiO <sub>2</sub> :Nd thin films. Polish Journal of Chemical Technology, 2015, 17, 103-111.	0.5	5
116	Coating of Tungsten Wire with Ni/Al Multilayers for Self-Healing Applications. Metals, 2017, 7, 574.	2.3	5
117	Improvement of Corrosion Resistance of 13CrMo4-5 Steel by Ni-Based Laser Cladding Coatings. Journal of Materials Engineering and Performance, 2020, 29, 3702-3713.	2.5	5
118	Characterization of Carbon Nanofibers/ ZrO2 Ceramic Matrix Composite. Archives of Metallurgy and Materials, 2013, 58, 459-463.	0.6	5
119	Analytical and HREM study of the early stages of SiO2–Al2O3–(Mg, Zn)O glass crystallisation. Materials Chemistry and Physics, 2003, 81, 411-413.	4.0	4
120	Scanning electron microscopy and transmission electron microscopy in situ studies of grain boundary migration in cold-deformed aluminium bicrystals. Journal of Microscopy, 2006, 223, 264-267.	1.8	4
121	TEM Analysis of Wear of Ti/TiN Multi-Layer Coating in Ball-on-Disc Test. Key Engineering Materials, 0, 409, 123-127.	0.4	4
122	Microstructure and Deposition Relations in Alumina Particle Strengthened Ni-W Matrix Composites. Solid State Phenomena, 2012, 186, 234-238.	0.3	4
123	On the wear of TiB x /TiSi y C z coatings deposited on 316L steel. International Journal of Materials Research, 2015, 106, 758-763.	0.3	4
124	Thermally Induced Crystallization of TiBx Thin Film after Deposition by Dual Beam IBAD Method. Materials Today: Proceedings, 2016, 3, 2646-2651.	1.8	4
125	Thermal characteristics and amorphization in plasma spray deposition of Ni-Si-B-Ag alloy. Journal of Alloys and Compounds, 2017, 710, 685-691.	5.5	4
126	Reactive resistance welding of Ti6Al4V alloy with the use of Ni(V)/Al multilayers. Physica Status Solidi - Rapid Research Letters, 2017, 11, 1600405.	2.4	4

#	Article	IF	CITATIONS
127	TEM investigations of wear mechanism of Al 2 O 3 and Si 3 N 4 compacts with GLPs additions. Ceramics International, 2017, 43, 8334-8342.	4.8	4
128	SEM/TEM Investigation of Aluminide Coating Co-Doped with Pt and Hf Deposited on Inconel 625. Materials, 2018, 11, 898.	2.9	4
129	Micro-analytical studies of discontinuous precipitation in Fe-13.5 at.% Zn alloy. Archives of Civil and Mechanical Engineering, 2020, 20, 1.	3.8	4
130	Interface Studies in HgTe/HgCdTe Quantum Wells. Physica Status Solidi (B): Basic Research, 2020, 257, 1900598.	1.5	4
131	(Ti,Al)O2 Whiskers Grown during Glow Discharge Nitriding of Ti-6Al-7Nb Alloy. Materials, 2021, 14, 2658.	2.9	4
132	Silicon based multilayer structures prepared by reactive pulsed laser deposition. Thin Solid Films, 1998, 318, 154-157.	1.8	3
133	Amorphization of the silicon substrate and stress-relaxation in HfN films bombarded with Au ions. Materials Science & Engineering A: Structural Materials: Properties, Microstructure and Processing, 1998, 253, 328-336.	5.6	3
134	Ordering of the β phase in TiNiCu and TiNiCuMn melt spun ribbons studied with the ALCHEMI technique. Materials Chemistry and Physics, 2003, 81, 230-232.	4.0	3
135	Structure and properties of an alumina/amorphous-alumina/platinum catalytic system deposited on FeCrAl steel. Journal of Microscopy, 2006, 224, 46-48.	1.8	3
136	Microstructure Characteristics of the Reaction Product Region Formed due to the High Temperature Contact of Molten Aluminium and ZnO Single Crystal. Solid State Phenomena, 0, 172-174, 1267-1272.	0.3	3
137	Structural properties of transparent Ti-V oxide semiconductor thin films. Open Physics, 2013, 11, .	1.7	3
138	TEM observations of reactive bonded Ti6Al4V alloy. Materials Letters, 2017, 189, 38-41.	2.6	3
139	Shear Strength of Reactive Resistance Welded Ti6Al4V Parts with the Use of Ni(V)/Al Multilayers. Metallurgical and Materials Transactions A: Physical Metallurgy and Materials Science, 2018, 49, 5423-5427.	2.2	3
140	On the morphological investigation of Pt dispersion and structure of alumina-platinum composites obtained by thermal oxidation of Al-Pt nano thin layers. Nano Structures Nano Objects, 2019, 17, 229-238.	3.5	3
141	Microstructure and properties of laser interference crystallized amorphous FeSiB ribbon. International Journal of Materials Research, 2019, 110, 11-17.	0.3	3
142	SHS reaction of Ti/Al multilayers and resistive heating used for joining of Ti-6Al-4V alloy. Materials Characterization, 2019, 154, 31-39.	4.4	3
143	Effect of Deposition Parameters on the Reactivity of Al/Ni Multilayer Thin Films. Coatings, 2020, 10, 721.	2.6	3
144	Formation of Nitrogen Doped Titanium Dioxide Surface Layer on NiTi Shape Memory Alloy. Materials, 2021, 14, 1575.	2.9	3

#	Article	IF	CITATIONS
145	A New Method for the Measurement of Thickness in Single Crystals. Micron, 1998, 29, 425-430.	2.2	2
146	Reactions and stresses in polycrystalline diamond-metal and diamond-carbide compacts. High Pressure Research, 2000, 18, 271-277.	1.2	2
147	Advances and problems with TEM characterization of Cr/CrN multilayer coatings. Journal of Microscopy, 2006, 223, 237-239.	1.8	2
148	Effect of Silicon Additions in CrSi (10, 20, 30, 40 at. % Si) Magnetron Targets on Microstructure of Reactively Deposited (Cr,Si)N Coatings. Solid State Phenomena, 2012, 186, 182-187.	0.3	2
149	TEM Investigation of Metal/Ceramic Interfaces in AA7475/AIN or Al <sub>2</sub> O <sub>3</sub> Nano-Composites. Solid State Phenomena, 2012, 186, 202-205.	0.3	2
150	Wetting Behavior and Reactivity Between AlTi6 Alloy and Carbon Nanotubes. Journal of Materials Engineering and Performance, 2016, 25, 3317-3329.	2.5	2
151	Ni-Cr-Ta-Al-C complex phase alloy – Design, microstructure and properties. Materials Science & Engineering A: Structural Materials: Properties, Microstructure and Processing, 2018, 711, 99-108.	5.6	2
152	Microstructure of Coatings on Nickel and Steel Platelets Obtained by Co-Milling with NiAl and CrB2 Powders. Materials, 2019, 12, 2593.	2.9	2
153	Microstructure Development in Multilayer TiB <sub>x</sub> /TiSi <sub>y</sub> C <sub>z</sub> Coatings during Post-Deposition Heat Treatment. Acta Physica Polonica A, 2016, 130, 1124-1126.	0.5	2
154	Nano-columnar, self-organised NiCrC/a-C:H thin films deposited by magnetron sputtering. Applied Surface Science, 2022, 591, 153134.	6.1	2
155	The Influence of Pd and Zr Co-Doping on the Microstructure and Oxidation Resistance of Aluminide Coatings on the CMSX-4 Nickel Superalloy. Materials, 2021, 14, 7579.	2.9	2
156	Sites are Separable in Garnets with ALCHEMI. Mikrochimica Acta, 2000, 132, 489-492.	5.0	1
157	Structure studies of ball-milled ZrCuAl, NiTiZrCu and melt-spun ZrNiTiCuAl alloys. Journal of Microscopy, 2006, 223, 268-271.	1.8	1
158	Scanning and transmission electron microscopy studies of the interface between the Tl-1223 phase and yttria doped zirconia substrates. Superconductor Science and Technology, 2006, 19, 493-496.	3.5	1
159	TEM investigation of reaction zone products formed between molten Al and CoO monocrystalline substrate. Journal of Microscopy, 2010, 237, 299-303.	1.8	1
160	HREM characterization of nanoâ€composite Au/SiO <sub>2</sub> layers. Journal of Microscopy, 2010, 237, 333-336.	1.8	1
161	TEM Investigation of Interfaces Formed between Saffil <sup>TM</sup> Fibers and AA6061 and En Ac 44200 Aluminium Alloys. Solid State Phenomena, 0, 186, 327-330.	0.3	1
162	SEM and TEM Microstructure Characterization of a Commercial Purity Aluminum after Laser Treatment. Solid State Phenomena, 0, 186, 323-326.	0.3	1

#	Article	IF	CITATIONS
163	Novel multilayer nano-composite protective coatings for metallic medical tools. International Journal of Materials Research, 2015, 106, 804-809.	0.3	1
164	Local Strengthening of EN AC-44200 Al Alloy with Ceramic Fibers. Key Engineering Materials, 0, 662, 237-240.	0.4	1
165	Microstructural Characterization of Nb/Inconel 601 Interface Obtained in the Explosive Welding Process. Microscopy and Microanalysis, 2021, , 1-8.	0.4	1
166	Microstructure of Ti/Al multilayer foils ignited with electric current. International Journal of Materials Research, 2019, 110, 60-65.	0.3	1
167	Microstructure, Thermal and Mechanical Properties of Refractory Linings Modified with Polymer Fibers. Ceramics, 2022, 5, 173-181.	2.6	1
168	Study of Garnets by ALCHEMI. Microscopy and Microanalysis, 2001, 7, 358-359.	0.4	0
169	Growth of PLD Hg 1-x Cd x Te films on Si-patterned substrates. , 2001, 4413, 55.		Ο
170	Defects formed within hardness indenter interaction zone in Al2O3?ZrO2composite. Journal of Microscopy, 2006, 223, 279-281.	1.8	0
171	Application of SEM/TEM to Tests on Pt Distribution in Al <sub>2</sub> 0 <sub>3</sub> Films Obtained by Oxidising FeCrAl Steel Foil Coated with Pt-Al Nanofilms. Advances in Science and Technology, 0, , .	0.2	Ο
172	Microstructure of LaNi <sub>5</sub> Base Nanopowders Produced by High Energy Ball Milling. Solid State Phenomena, 2012, 186, 124-129.	0.3	0
173	Effect of Heating on the Microstructure of NiAl + CrB2 Coatings Deposited by Mechanical Embedding in a Ball Mill. Microscopy and Microanalysis, 0, , 1-5.	0.4	Ο
174	Development of Actuators for Repairing Cracks by Coating W Wires with Reactive Multilayers. Materials, 2022, 15, 869.	2.9	0
175	TEM Observations of the Microstructural Changes in the Interfacial Zone of Explosively Welded Titanium/Steel Before and After <i>Ex Situ</i> and <i>In Situ</i> Heat Treatment. Microscopy and Microanalysis, 2022, , 1-8.	0.4	Ο